3.3 THE GLOBAL OCEAN DATA ASSIMILATION SYSTEM (GODAS) AT NCEP

David W. Behringer*
NOAA/NCEP/Environmental Modeling Center

1. INTRODUCTION

Beginning more than 10 years ago the National Centers for Environmental Prediction (NCEP) has employed coupled ocean-atmosphere numerical models for making seasonal to interannual (S-I) climate forecasts in an operational or quasi-operational mode (Ji et al., 1995; Ji et al., 1998; Saha et al., 2005). A critical element of the forecast effort is an ocean data assimilation system (ODAS) that provides an estimate of the ocean state to initialize the coupled forecasts. The original ODAS was based on the Geophysical Fluid Dynamics Laboratory (GFDL) Modular Ocean Model version 1 (MOM.v1) and was configured for the Pacific Ocean (Ji et al., 1995). The data assimilation method was a three-dimensional variational (3DVAR) scheme devised by Derber and Rosati (1989). The Pacific ODAS was later modified to incorporate revised background error covariances (Behringer et al. 1998) and to assimilate satellite altimetry data (Vossepoel and Behringer, 2000; Ji et al., 2000).

Over the last few years a new Global Ocean Data Assimilation System (GODAS) was developed to be the replacement for the Pacific ODAS, and to provide the oceanic initial conditions for the new NCEP coupled Climate Forecast System (CFS). The GODAS became operational in 2003 and the CFS went operational in 2004. A description of the GODAS is provided by Behringer and Xue (2004). The purpose here is to describe the impact on the standard or operational GODAS of subsequent developments, both in terms of the data sets that are assimilated and of modifications to the methodology. Specifically, we will first look at the separate impacts of assimilating satellite altimetry data and Argo salinity profiles and then consider the separate effects of deepening the range of the assimilation and of modifying the assimilation method to be multivariate in velocity. The report begins with a short description of the standard GODAS, turns next to sections describing the assimilation of altimetry data and salinity, continues with sections on the deep and multivariate assimilations and finishes with some overall conclusions based on the results.

* *Corresponding author:* David W. Behringer, NOAA/NCEP Environmental Modeling Center, W/NP23, 5200 Auth Rd., Camp Springs, MD, 20746, USA; e-mail: david.behringer@noaa.gov

2. THE STANDARD OPERATIONAL GODAS

2.1 The Model

The GODAS is based a quasi-global configuration of the GFDL MOMv3 (Pacanowski and Griffies, 1998). The model domain extends from 75^{O}S to 65^{O}N and has a resolution of 1^{O} by 1^{O} enhanced to $1/3^{O}$ in the N-S direction within 10^{O} of the equator. The model has 40 levels with a 10 meter resolution in the upper 200 meters. This configuration represents a small improvement over the Pacific ODAS which had a 1.5^{O} resolution in the E-W direction and 28 levels in the vertical. Other new features include an explicit free surface, the Gent-McWilliams isoneutral mixing scheme and the KPP vertical mixing scheme. The GODAS is forced by the momentum flux, heat flux and fresh water flux from the NCEP atmospheric Reanalysis 2 (R2) (Kanamitsu et al. 2002). In addition the temperature the top model level is relaxed to weekly analyses of sea surface temperature (Reynolds et al., 2002), while the surface salinity is relaxed to annual salinity climatology (Conkright et al., 1999). Very short relaxation periods are used (5 days for temperature and 10 days for salinity). The GODAS assimilates temperature profiles and, in another new feature, assimilates synthetic salinity profiles as well. The assimilation method is the same 3DVAR scheme used in the Pacific ODAS, but it has been modified to assimilate salinity and the code has been rewritten to run in a multi-processor computing environment.

2.2 The Standard Assimilation Dataset

The standard GODAS assimilates temperature profiles from XBTs, from TAO, TRITON and PIRATA moorings (McPhaden et al., 2001) and from Argo profiling floats (The Argo Science Team, 2001). At NCEP, XBT observations collected prior to 1990 have been acquired from the NODC World Ocean Database 1998 (Conkright et al., 1999), while XBTs collected subsequent to 1990 have been acquired from the Global Temperature-Salinity Profile Project (GTSPP). In addition, a synthetic salinity profile is computed for each temperature profile using a local T-S climatology based on the annual mean fields of temperature and salinity from the NODC World Ocean Database (Conkright et al., 1999). Figure 1 shows the monthly number of temperature profiles used in GODAS. The number of profiles can vary significantly from month to month, but there are longer term trends as well. For example, there is a gradual decline in the monthly counts after 1985 followed by a sharp recovery in 1990 when the source of the profiles changed.

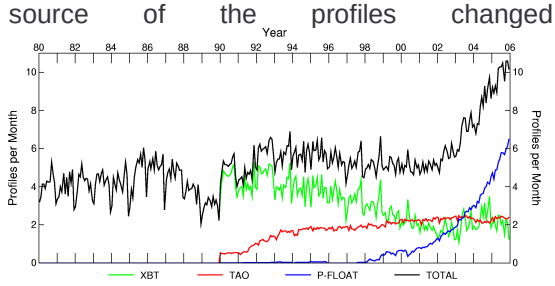

Figure 1. Monthly number of temperature profiles used in GODAS. Numbers are thousands of profiles.

There are also changes in the nature and distribution of the profiles. For example, the TAO moorings represent a fixed array of daily observations in the tropical Pacific Ocean that has no counterpart in the 1980s. More recently the rapid growth of the Argo network represents both an important increase in the number of profiles and a departure from the older XBT network for which the profiles are confined to ship tracks. Figure 2 gives some flavor of the changes in the geographical distribution of the profiles. The complete dependence on XBT profiles in the 1980s left large parts of the global ocean uncovered. The arrival of the TAO array in the 1990s and the rapid expansion of the Argo array between 2000 and 2005 changed the fundamental nature of the data set and by 2005 had greatly improved the coverage of the southern hemisphere. These changes in the data suite will have an impact on the GODAS analysis.

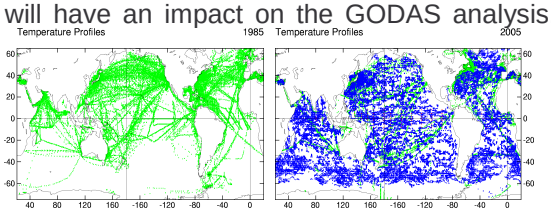

Figure 2. The distribution of temperature profiles in 1985 (l.) and 2005 (r.).

2.3 The Performance of the Operational GODAS

The operational GODAS has been used for a long reanalysis extending from 1980 to the present. The results of that reanalysis will be the basis for the comparisons in the subsequent sections. However, in the meantime, Figures 3 and 4 can provide a

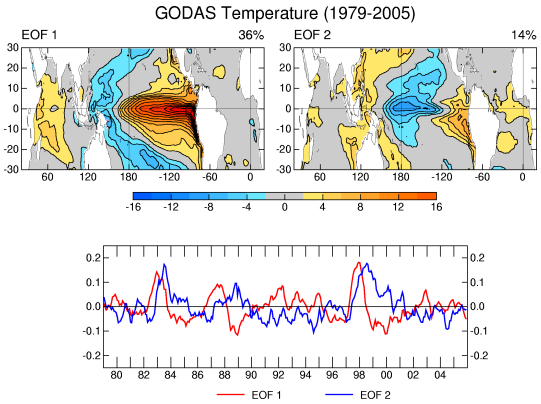

Figure 3. The first two EOFs of anomalous monthly SST from the standard GODAS.

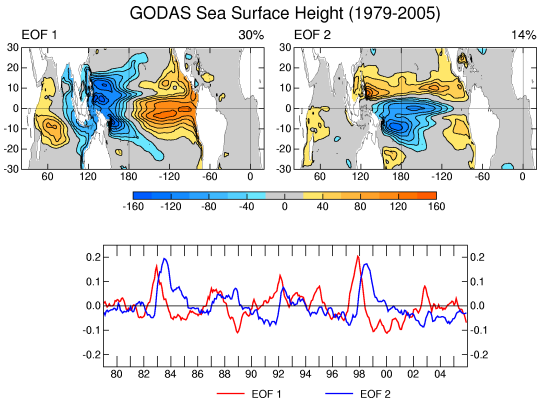

Figure 4. The first two EOFs of anomalous monthly SSH from the standard GODAS.

general sense its performance. Figure 3 shows the first two EOFs of the monthly averaged anomalous SST from the reanalysis. The patterns in the EOFs are the familiar ones associated with El Nino / La Nina and the time series clearly capture the events of the past 25 years. Figure 4 shows the first two EOFs for the anomalous sea surface height (SSH) and the El Nino / La Nina patterns are dominant. In short, the operational GODAS is well constrained by temperature and synthetic salinity data and is capable of reproducing the ENSO phenomenon necessary for S-I forecasting.

3. THE ASSIMILATION OF SATELLITE ALTIMETRY DATA

3.1 Modifications to the Assimilation Scheme

The standard GODAS 3DVAR scheme is essentially the same as the original Derber and Rosati (1989) scheme, although it has been adapted to assimilate salinity in addition to temperature. In order to assimilate sea surface height (SSH) observations further modifications are necessary. These same modifications were made earlier to the Pacific ODAS and are described in Behringer et al. (1998) and Ji et al. (2000), but will be covered briefly here as well. The modified 3DVAR scheme minimizes a functional,

$$\mathbf{I} = \tfrac{1}{2}\{\mathbf{T}^{\mathrm{T}}\mathbf{E}^{-1}\mathbf{T}\} + \tfrac{1}{2}\{[D(\mathbf{T}) - \mathbf{T}_0]^{\mathrm{T}}\mathbf{F}^{-1}[D(\mathbf{T}) - \mathbf{T}_0] + [D(L\mathbf{T}) - \delta\mathbf{Z}_0]^{\mathrm{T}}\mathbf{G}^{-1}[D(L\mathbf{T}) - \delta\mathbf{Z}_0]\}$$

where the vector **T** represents the correction to the first-guess prognostic tracers (temperature and salinity) computed by the model, **E** is the first guess error covariance matrix, $\mathbf{T}_0$ represents the difference between the tracer observations and the first-guess, *D* is an interpolation operator that transforms the first-guess tracers from the model grid to the observation locations, **F** is the observation error covariance matrix for the tracers, *L* is a linear operator that transforms a vertical column of temperature and salinity corrections into an estimate of the correction to the first-guess dynamic height field, **G** is the observation error covariance matrix for SSH, and $\delta\mathbf{Z}_0$ represents the difference between the observed and first-guess SSH fields. The observational errors are assumed to be uncorrelated, so the matrices, **F** and **G**, have only diagonal elements, which are the error variances of the observations. The last term on the right-hand side is a constraint imposed by the observed SSH. It would be pointless to correct the model SSH directly; instead, the SSH observations are used to impose an integral vertical constraint on the corrected model temperature and salinity fields. The relative magnitudes of these corrections throughout the water column depend on the vertical structure of the first-guess error covariance matrix. In other words, the assimilation system preferentially corrects the model temperature and salinity where their expected errors are greatest, making those corrections in such a way as to bring the model surface dynamic height into closer agreement with the SSH observations. An implied assumption in this approach is that we can use the SSH observations to correct only the baroclinic part of the model SSH and that it is safe to neglect the barotropic part. In the Tropics, our main region of interest, this may be a reasonable assumption.

The 3DVAR scheme avoids the problem of knowing the absolute SSH by assimilating only the variable part of the SSH and so in the minimization of the cost function the altimetry data and first-guess model SSH data each have their own long-term mean removed. In the case of the model data a 1993–99 seven-year mean is computed from the output of the standard GODAS reanalysis.

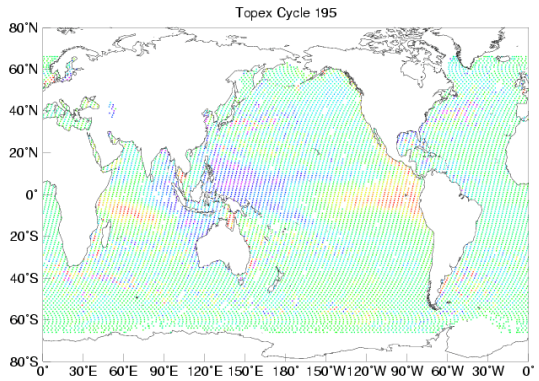

Figure 5. Along track SSH data from TOPEX (cycle 195) as used in GODAS.

3.2 The Altimetry Experiment

The altimetry experiment assimilates a merged TOPEX and Jason-1 dataset and runs

from 1993 through 2005. In these experiments only the data between 30°S and 40°N were assimilated. The data sets were provided by the AVISO SSALTO/DUACS as two internally consistent time series of sea surface height deviations, relative to a 1993–99 seven-year mean. The TOPEX/Jason data were corrected based on internal crossovers to remove residual orbit error, and to ensure compatibility between missions (Le Traon and Ogor, 1998; Lillibridge et al., 2005). Figure 5 shows an example of the along-track data at the time of the 1997-98 El Nino as they are assimilated into the GODAS.

While the period 1993-2005 includes important changes in the basic observational suite, the Tao array remains relatively constant and the abrupt discontinuity in 1990 in the XBT distribution is avoided. Also the rapid growth in the Argo network after 2000 took place globally, while the rate at which observations were made in the tropics remained relatively constant.

The results of the altimetry experiment are compared to the satellite altimetry data itself and to independent island tide gauge data. To evaluate the impact of the altimetry data on the GODAS, the same comparisons will be made using the results from the standard GODAS reanalysis and, in the case of the tide gauge data, from a Control run of the ocean model that is forced by the same R2 data, but that does not assimilate any observations.

3.3 Comparisons of GODAS SSH with Satellite Altimetry

For the purpose of these comparisons a simple OI scheme was used to make monthly maps of the TOPEX/Jason satellite altimetry on the GODAS grid. The maps represent monthly anomalies of SSH from the 1993-99 mean. The maps were compared to the monthly average SSH anomalies from the standard GODAS analysis and the GODAS analysis that assimilates the TOPEX/Jason data. Figure 6 shows the correlations and RMS differences between the observations and the model results for the period 1993-2005. In the top two panels, the standard GODAS, assimilating temperature and synthetic salinity, shows the impact of the TAO array in the Pacific where there is a broad band of correlations greater than 0.8 and RMS differences less than 3 cm. The correlations are weak in the Indian Ocean and weaker yet in the Atlantic Ocean where the interannual signal is small. This is a reflection of the relatively poorer distribution of assimilation data in the Indian Ocean as compared with the Pacific and Atlantic Oceans. Finally, in the bottom panels the GODAS analysis that assimilates the satellite SSH data is compared with that same data. The assimilation of the

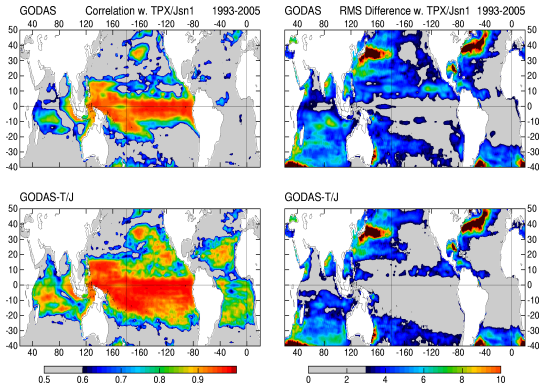

Figure 6. Anomaly correlations and RMS differences between GODAS SSH and TOPEX/Jason-1. Top: standard GODAS. Bottom: GODAS assimilating TOPEX/Jason-1.

SSH data has resulted in broad improvements in the model SSH. Correlations are 0.6 or better almost everywhere within 30 degrees of the equator. The RMS differences of model SSH with observations are less than 3 cm over large portions of the Atlantic and Pacific. In the tropics the RMS differences remain somewhat larger (4-5 cm) in the region of the tropical instability waves and the recirculation of the Brazil current.

3.4 Comparisons with Island Tide Gauges

We next compare the model output with island tide gauge data. Here we also include a Control model run that does not assimilate any data. The tide gauge data are not assimilated and are thus independent of all the model runs. Research quality tide gauge data were acquired from the University of Hawaii Sea Level Center in the form of monthly average SSHs. The time-series are shown in Figure 7 for the tide gauge SSHs and the model SSHs interpolated to the gauge locations. Each time-series has its own mean removed. The RMS differences and correlations for each tide gauge / model pair are listed in Table 1. The gauges shown in Figure 7a are near or outside the margins of the TAO array in the western Pacific. The

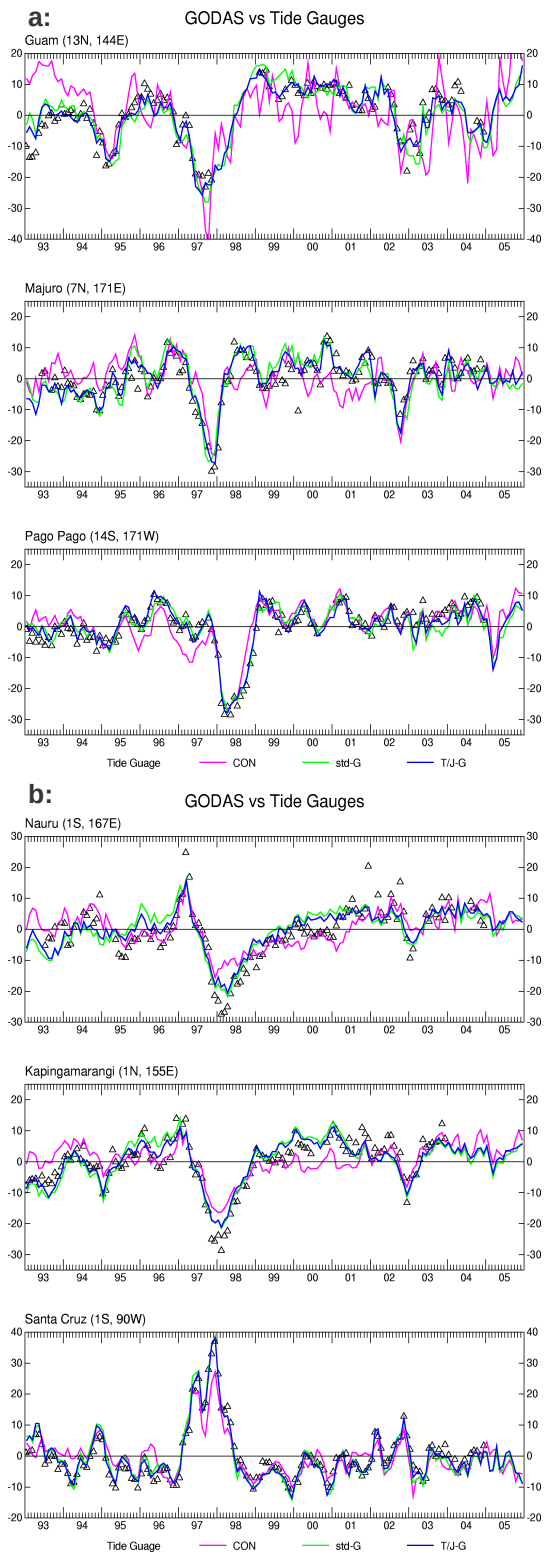

Figure 7. Anomalous GODAS SSH vs. island tide gauges. a: Locations outside the TAO array. b: Locations within the TAO array.

Control captures the large events, but it also has large departures from the tide gauge records, most noticeably at Guam. The assimilation of temperature and salinity largely corrects the standard GODAS analysis and the assimilation of altimetry SSH data corrects the GODAS analyses even further. For these latter analyses the RMS errors are 2-3 cm and the correlations with the tide gauge SSH exceed 0.9 (Table 1). Figure 7b shows three gauges that are within one degree of the equator, two in the western Pacific and one in the Galapagos in the eastern Pacific. For this group the SSH in the Control is closer to the SSH in the three GODAS analyses, even capturing the double peak of the 1997 El Nino and some of the subsequent small variations at the Galapagos. In the western Pacific none of the model runs capture the extreme amplitudes of the 1997 event. They also miss several questionable small spikes in the 2001-02 tide gauge records at the two western sites. At the Galapagos site all three GODAS analyses perform very well; the RMS errors are 2-3 cm and the correlations exceed 0.95 (Table 1). At Limetree Bay in the Atlantic basin the standard deviation of the tide gauge time-series is about half the magnitude of the standard deviations at the Pacific sites and the correlations between the tide gauge SSHs and the model SSHs are lower here than at the Pacific sites. Nevertheless, the model runs do capture the three large oscillations in the tide gauge record between 1993 and 2001

4. THE ASSIMILATION OF ARGO SALINITY DATA

4.1 The Salinity Experiment

The experiment, GODAS-A, was conducted for the period 2000-2005. During this period the number of Argo temperature profiles increased from 700 profiles / month to 4600 profiles / month, while the number of salinity profiles increased from 160 profiles / month to 4400 profiles / month. At the same time the total number of XBT and mooring profiles grew from about 4400 profiles / month to about 5900 profiles / month. Thus, over the course of the experiment, while the absolute number of observed salinity profiles grew by a factor of 30, the percentage of observed salinity profiles grew more slowly from 3% of the total to about 40%.

Table 1. Tide Gauge vs Model Statistics (RMS of differences in cm)				
Location (TG std.dev. in cm)		Control	Std GODAS	T/J GODAS
		1993-2005*		
Guam (8.66) 13-26N, 144-39E	RMS	9.62	4.41	3.11
	COR	0.53	0.88	0.93
Majuro (6.98) 07-07N, 171-22E	RMS	6.34	4.50	3.25
	COR	0.54	0.81	0.93
Pago Pago (7.80) 14-17S, 170-41W	RMS	4.71	3.06	2.27
	COR	0.81	0.92	0.96
Nauru (8.98) 00-32S, 166-55E	RMS	5.04	5.04	4.33
	COR	0.84	0.83	0.89
Kapingamarangi (8.28) 01-06N, 154-47E	RMS	4.97	3.73	3.14
	COR	0.82	0.90	0.93
Santa Cruz (8.50) 00-45S, 090-19W	RMS	4.23	2.52	2.03
	COR	0.87	0.96	0.97
Limetree (3.73) 17-42N, 064-45W	RMS	3.68	3.59	2.68
	COR	0.38	0.66	0.74

Table 1. Comparison of a Control experiment (no assimilation), the standard GODAS and a version of GODAS assimilating altimetry with independent tide gauges. (Record lengths may vary due to gauge data dropouts).

The standard GODAS assimilates synthetic salinity profiles that are paired with each temperature profile. Therefore no changes were made to the assimilation scheme; however several changes were made to the assimilation data set. First, the synthetic salinity profiles associated with Argo temperature profiles were replaced with observed salinity profiles. If an Argo temperature profile was missing an associated observed salinity profile, the synthetic profile was retained. The synthetic profiles associated with XBT profiles were also retained. Second, the TAO mooring profiles and their associated synthetic salinity profiles were not assimilated. This was done to avoid undue influence from synthetic salinity in the tropical Pacific. Finally, before combining the synthetic and observed salinity profiles in a single experiment, we used the differences between co-located observed and synthetic salinity profiles to apply a calibration to the synthetic profiles and to increase the representation errors assigned to them. To do this we first binned the observed minus synthetic profile differences into 5^o latitude by 10^o longitude boxes and computed the mean and RMS differences. These results were then mapped onto the model grid. Figure 8 shows slices from these fields at the surface and in an equatorial section. As might be expected, the differences are large in the surface layers and in geographic locations where the assumption of a stable TS-relationship that underlies the synthetic salinity profiles is most likely to break down. These data were further interpolated to

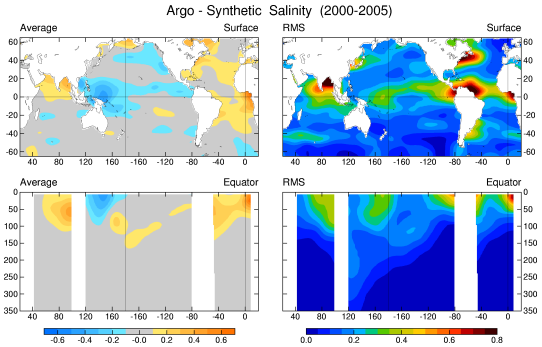

Figure 8. Mean and RMS differences between the observed Argo salinity and the synthetic salinity that is used in the standard GODAS.

the positions of the synthetic profiles where the mean difference was added to the synthetic profile and the square of the RMS difference was added to the square of a background observation error. A background observation error is assigned to all salinity profiles, synthetic and observed alike, and is intended to account for the mismatch between what is measured by a single profile and what can be resolved by the numerical model. In this experiment, as in the standard GODAS, the background error for salinity is assigned the global value of 0.1 psu.

4.2 Comparison of the Salinity Experiment with the Standard GODAS

Figure 9 shows the mean differences between the GODAS-A and the standard GODAS for the year 2005 at the surface and in an equatorial section. The patterns and magnitudes of the differences are comparable

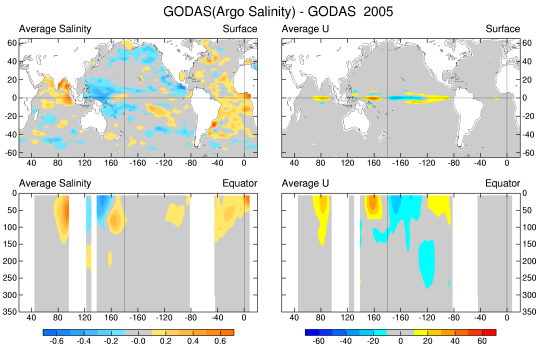

Figure 9. Mean differences in salinity and zonal velocity between the GODAS assimilating Argo salinity and the standard GODAS.

to errors in the synthetic salinity data that are shown in Figure 8, demonstrating the positive impact of the Argo salinity data on the GODAS-A. The right hand side of Figure 9 shows the impact of the Argo salinity on the mean equatorial zonal flow, such that the near surface flow has become more eastward in the western and eastern Pacific and more westward in the central Pacific by as much as 10-30 cm/sec.

4.3 Comparison the GODAS Experiments with Independent ADCP Data

The GODAS results have been compared with acoustic Doppler current profile (ADCP) data at four TAO locations on the equator: 165°E, 170°W, 140°W, and 110°W. The comparisons are of mean profiles for the year 2005 when the Argo salinity are most numerous and dominate the analysis. Figure 10a shows the results for the two eastern locations. At 110°W, GODAS-A (red) agrees more closely with the observed ADCP profile below the undercurrent maximum than does the standard GODAS (blue). At 140°W, GODAS-A does better above the current maximum while the standard GODAS does

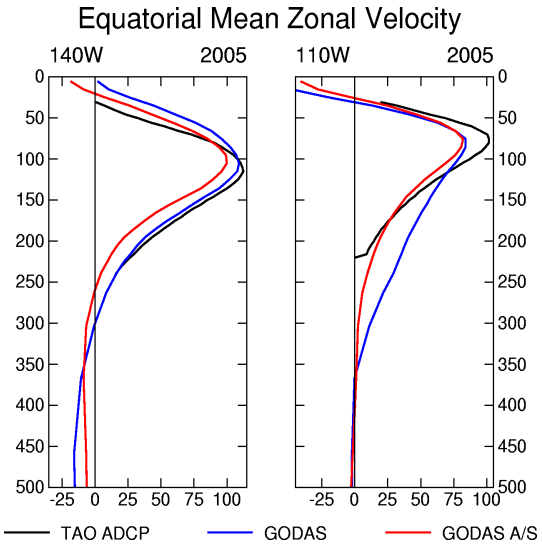

Figure 10a. The mean zonal velocity from ADCP data, the standard GODAS and the GODAS assimilating Argo salinity on the equator at 140°W and 110W for the year 2005.

better at and below the maximum. The most remarkable results are for the two western locations shown in Figure 10b. At both 165°E and 170°W, GODAS-A clearly outperforms GODAS. At both locations, GODAS-A captures almost perfectly the unusual structures of the observed currents.

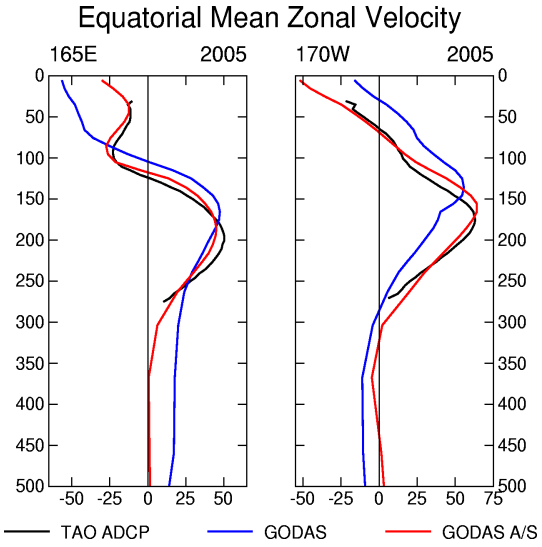

Figure 10b. The mean zonal velocity from ADCP data, the standard GODAS and the GODAS assimilating Argo salinity on the equator at 165°E and 170W for the year 2005.

5. THE DEEP GODAS EXPERIMENT

5.1 The Experiment

A long analysis (1980-2005) with a version of the GODAS was done that extended the depth of the data assimilation from the operational standard of 750 meters to 2200 meters. The idea behind the experiment was to see whether it is possible to take advantage of the new deep Argo profiles in the context of a long multi-decade analysis. In order to do a deep assimilation in the first 20 years of the experiment we blended the 450 meter XBTs (dominant in the 1980s) and the 750 meter XBTs (dominant in the 1990s) with deeper climatological data. It is clear that this strategy will not capture deep variability; the intent, instead, is to correct model bias in the early years and thus set the stage for making use of the growing number of deep Argo profiles after 2000.

5.2 Comparison of the Deep experiment with the Standard GODAS

Figure 11 shows temperature at 1200 meters depth on the equator as a longitude vs. time plot for the two versions of GODAS. In

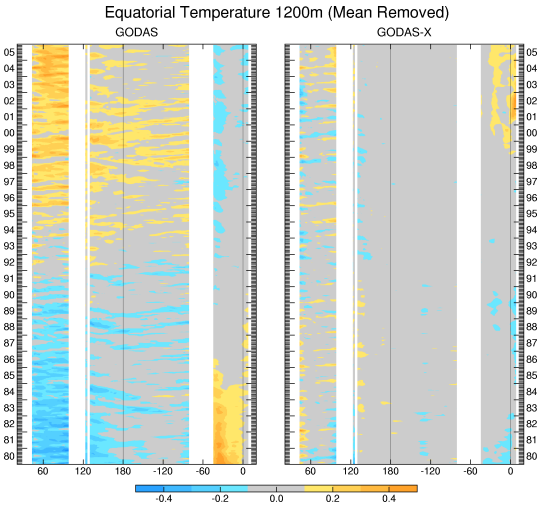

Figure 11. Time vs. Longitude plot of equatorial temperature at 1200 meters in the standard GODAS (l.) and the deep assimilation version

the operational GODAS (left panel), there is a drift toward warmer temperatures in the Indian and Pacific Oceans and toward colder temperatures in the Atlantic Ocean. In the GODAS experiment with deep assimilation (right panel), the temperature drifts in the Indian and Pacific Oceans have been eliminated. The cold drift in the Atlantic Ocean has been replaced by a long-term warming trend.

5.3 Comparison the GODAS Experiments with Independent CTD Data

Figure 12 shows in the top two panels two CTD sections along the A16 line in the Atlantic Ocean, one occupied in 1988 and 1989 as part of the WOCE field program (left) and one occupied in 2003 and 2005 by the NOAA Pacific Marine Environmental Laboratory.

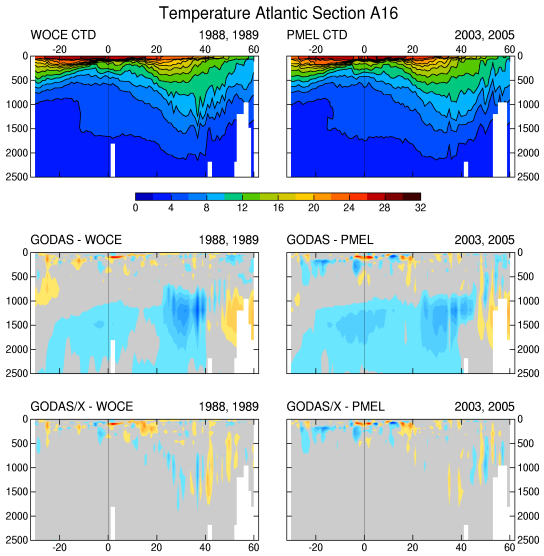

Figure 12. The standard GODAS (m.) and the deep assimilation version of GODAS (b.) compared with CTD sections along the Atlantic WOCE A16 line

The middle and bottom panels show the differences between the GODAS analyses and the A16 CTD sections. In the operational GODAS (middle panels), the water at 1000-2000 meters below the depth of the standard assimilation depth is too cold. The largest differences are 1-2^{o}C in the North Atlantic. In the deep GODAS experiment that assimilates data down to 2200 meters (bottom panels), the cold bias has been corrected and, by implication, the warm trend in the mid-waters of that experiment is also correct (Figure 11, right-hand side).

6. THE MUTIVARIATE GODAS EXPERIMENT

6.1 Modifications to the Assimilation Scheme

The standard GODAS assimilation scheme is univariate in temperature and salinity and relies on the ocean model to adjust the velocity field to the temperature and salinity corrections. A paper of Burgers et al. (2002) suggests that the equatorial circulation could be improved by an assimilation that balances temperature and salinity corrections with velocity corrections based on the geostrophic relationship. For this experiment the balance was imposed by replacing the standard univariate background error covariance matrix in the assimilation scheme with a multivariate matrix.

6.2 The Experiment

A short multivariate experiment, GODAS-M, was done for the period 2000-2005. This experiment represents an early stage in the refinement of the technique. Care must be taken with how the method is applied close to the equator. One issue is that the standard geostrophic relationship breaks down at the equator and a decision must be made on how to compute velocity corrections across the equator. In the present experiment, the corrections at 1°S and 1°N are interpolated to grid points across the equator. Another issue is that equatorial undercurrent is not entirely in geostrophic balance and at this stage it appears that in the equatorial zone the method works best when it is applied only to the near surface velocity. In this experiment that has been achieved by a mask that prevents velocity corrections from being applied to the undercurrent. The same effect could be attained through the design of the multivariate matrix.

6.3 The GODAS Experiments Compared to Independent ADCP Data

The GODAS results have been compared with ADCP data at the same four equatorial TAO locations as used in Section 4 on the Argo salinity experiment, 165°E, 170°W, 140°W, and 110°W. Figure 12a shows the mean of the zonal velocity for the year 2005 in the eastern Pacific. At 110°W, there is little

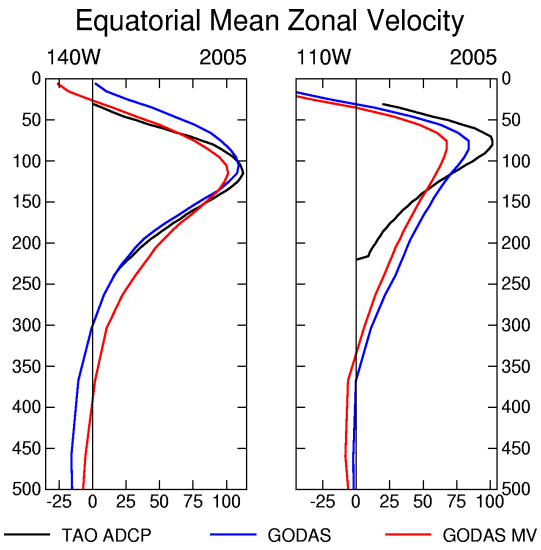

Figure 12a. The mean zonal velocity from ADCP data, the standard GODAS and the multivariate GODAS on the equator at 140°W and 110W for the year 2005.

difference between the multivariate GODAS-M and the standard GODAS. At 140°W, however, GODAS-M successfully corrects the mean eastward bias near the surface in the standard GODAS. Below the maximum of the

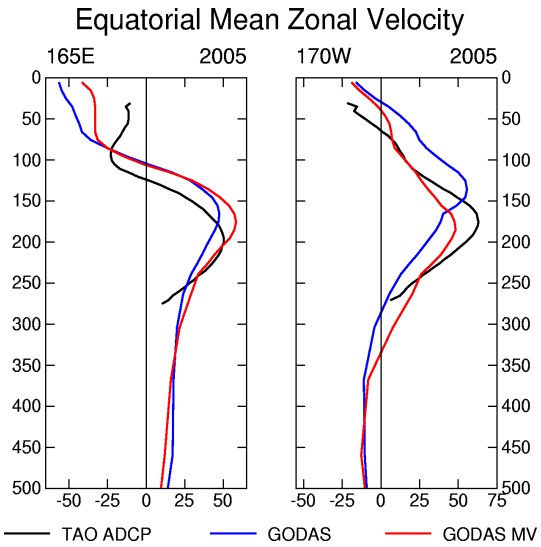

Figure 12b. The mean zonal velocity from ADCP data, the standard GODAS and the multivariate GODAS on the equator at 165°E and 170W for the year 2005.

undercurrent the GODAS-M does less well, actually degrading the analysis slightly. In the results for the western Pacific, shown in Figure 12b, GODAS-M performs slightly better than the standard GODAS, although not in a

consistent fashion. At 165°E, GODAS-M partially corrects the eastward bias in the surface current of the standard GODAS. At 170°W, GODAS-M does a better job than GODAS with respect to the depth of the maximum current and has less eastward bias in the current above the maximum. Further improvements through the use of a multivariate assimilation may be possible with further refinement of the technique.

7. SUMMARY AND DISCUSSION

A consistent, uninterrupted altimetry data set (TOPEX/Jason-1) has been available since late 1992, providing a good basis for testing its impact on GODAS. In the equatorial Pacific the assimilation of the TAO mooring and other profile data alone leads to a good representation of the anomalous SSH in the operational GODAS. Nevertheless, the addition of the TOPEX/Jason-1 altimetry to the assimilation data set improves GODAS SSH beyond the bounds of the TAO array and well into the subtropics. In the tropical Pacific, comparisons with independent tide gauge data show that the assimilation of the altimetry date improves the anomalous SSH in GODAS consistently by about 30% outside the bounds of the TAO array and by 15-20% within the array. In the Atlantic and Indian Oceans the operational GODAS does a relatively poor job representing the SSH anomaly field. In these two oceans the assimilation of altimetry greatly improves GODAS SSH.

In the GODAS-A experiment, the assimilation of the Argo salinity data, which are not part of the operational GODAS data set, produces significant changes in the GODAS-A salinity field that are consistent with the differences between the observed Argo salinity and the synthetic salinity used in the standard GODAS. The salinity differences are largest in the surface layers where the forcing is most variable and the notion of a stable T-S relationship, which is the basis of the synthetic salinity, breaks down. Associated with the changes in salinity are changes in the mean currents of the tropical oceans. In the Pacific, these changes represent remarkable improvements over the currents in the standard GODAS. In the western equatorial Pacific, the currents in GODAS-A reproduce the complicated vertical structure of the observed currents with great fidelity.

In the last few years the Argo array has largely replaced the XBT network as the primary source of global subsurface temperature data. It is also an unprecedented source of subsurface salinity data. As of this writing, there are 2573 Argo floats deployed, representing over 85% of the planned 3000 floats worldwide. The extension of the assimilation from a depth of 750 m in the operational GODAS to a depth of 2200 m eliminates the erroneous temperature drifts in the deep (1000-2000m) Indian, Pacific, and Atlantic Oceans that are present in the standard GODAS. A comparison of the deep assimilating GODAS with two sections of independent CTD observations, collected at an interval of 25-years along the Atlantic WOCE A16 line, shows that a cold bias of 2-3°C in the standard GODAS has been effectively eliminated.

The multivariate GODAS-M experiment was conceived as a possible solution to the eastward mean bias in the surface equatorial current of the standard univariate GODAS. The multivariate GODAS-M applies current corrections that are in partial geostrophic balance with the temperature and salinity corrections and succeeds in reducing the eastward bias in the surface currents.

The most surprising result that has come out of this group of experiments is that the univariate GODAS-A, assimilating observed salinity, does a much better job with the equatorial Pacific currents than the multivariate GODAS-M. Other differences between the two experiments are that GODAS-M assimilates only synthetic salinity and also assimilates the TAO profile data that are left out of GODAS-A. These experiments are short, but pending more extensive results, the implication is that it may be more important to do a good analysis of the salinity field (and therefore the mass field) than to do a balanced multivariate assimilation. The results of another univariate experiment support this speculation. This experiment, which has not been discussed previously in this paper, assimilates the Argo salinity profiles, but also assimilates the TAO temperature and synthetic salinity profiles. The tropical currents in this experiment again have an eastward bias and are nearly identical to those in the standard GODAS. The advantage gained from assimilating Argo salinity in GODAS-A has been lost in this experiment, apparently swamped by too much synthetic

salinity data. One clear message here is that a better job must be done with synthetic salinity. There are two obvious reasons. First, only in the last year or so has there been enough Argo salinity data to support an analysis like GODAS-A. Second, leaving TAO data out of the analysis is not a realistic option. Some work has already been done on synthetic salinity in the tropical Pacific (e.g. Maes and Behringer, 2000) and it may be worth some re-examination.

In conclusion, there a few general remarks that are important to keep in mind.

1) The standard operational GODAS already does a good job in the tropical Pacific assimilating only temperature and synthetic salinity.

2) The success of the standard GODAS in the equatorial Pacific is, in large part, due to the TOGA-TAO mooring array.

3) Although the assimilation of TOPEX/Jason-1 improves the anomalous SSH in GODAS in RMS terms consistently by about 30% outside and 15-20% within the bounds of the TAO array, this represents only about 0.5-1.5 cm in absolute terms. The primary purpose of GODAS is to provide initial conditions for S-I forecasts and it is not yet known whether improvements on this order will lead to improvements in the forecasts.

4) The added value of the Argo array in recent years can only help in the 1980s or 1990s though possible improvements to temperature and salinity climatologies. Long GODAS analyses extending back at least to 1980 are needed to initialize the retrospective forecasts used to current S-I forecasts.

These and other improvements will become part of the next version of GODAS and will contribute to a better representation of the ocean state. How and whether this improved ocean state will contribute to improved S-I forecasting at NCEP will only be known after an extensive series of retrospective forecasts are completed.

Acknowledgements: The Argo data were collected and made freely available by the International Argo Project and the national programmes that contribute to it. Argo is a pilot programme of the Global Ocean Observing System. The altimeter products were produced by Ssalto/Duacs as part of the Environment and Climate EU Enact project (EVK2-CT2001-00117) and distributed by Aviso, with support from Cnes. The tide gauge data are available from the University of Hawaii Sea Level Center.

9. References

Argo Science Team, 2001: The global array of profiling floats. *Observing the Ocean in the 21st Century.* C. J. Koblinsky and N. R. Smith, Eds., Australian Bureau of Meteorology, 248–258.

Behringer, D.W., M. Ji, and A. Leetmaa, 1998: An improved coupled model for ENSO prediction and implications for ocean initialization. Part I: The ocean data assimilation system. *Mon. Wea. Rev*., **126**, 1013-1021.

Behringer, D.W., and Y. Xue, 2004: Evaluation of the global ocean data assimilation system at NCEP: The Pacific Ocean. *Eighth Symposium on Integrated Observing and Assimilation Systems for Atmosphere, Oceans, and Land Surface, AMS 84th Annual Meeting, Washington State Convention and Trade Center, Seattle, Washington, 11-15*.

Burgers, G., M. A. Balmaseda, F. C. Vossepoel, G. J. van Oldenborgh, and P. J. van Leeuwen, 2002: Balanced ocean data assimilation near the equator, J. Phys. Oceanogr., 32, 2509-2519.

Conkright, M.E., S. Levitus, T. O'Brien, T.P. Boyer, C. Stephens, D. Johnson, O. Baranova, J. Antonov, R. Gelfeld, J. Rochester, C. Forgy, 1999: World Ocean Database 1998, Documentation and Quality Control Version 2.0, National Oceanographic Data Center Internal Report 14, National Oceanographic Data Center, Silver Spring, MD.

Derber, J.C., and A. Rosati, 1989: A global oceanic data assimilation system. *J. Phys. Oceanogr*., **19**, 1333-1347.

Ji, M., A. Leetmaa, and J. Derber, 1995: An ocean analysis system for seasonal to interannual climate studies. *Mon. Wea. Rev*., **123**, 460-481.

Ji, M., R.W. Reynolds, and D.W. Behringer, 2000: Use of TOPEX/Poseidon sea level data for ocean analyses and ENSO prediction: Some early results. *J. Climate*, **13**, 216-231.

Ji, M. D.W. Behringer, and A. Leetmaa, 1998: An improved coupled model for ENSO prediction and implications for ocean initialization. Part II: The coupled model. *Mon. Wea. Rev*., **126**, 1022-1034.

Kanamitsu, M., W. Ebisuzaki, J. Woolen, S.-K. Yang, J.J. Hnilo, M. Fiorino, and G.L. Potter, 2002: NCEP-DOE AMIP-II reanalysis (R-2). *Bull. Amer. Meteor. Soc*., **83**, 1631-1643.

Lillibridge, J., D. Behringer, Y. Xue and J. Kuhn, 2005: Improving ocean analyses and ENSO forecasts at NOAA using the global ocean data assimilation system and altimetric sea level

Le Traon, P.-Y., and F. Ogor, 1998: ERS-1/2 orbit improvement using TOPEX/Poseidon: the 2 cm challenge, J. Geophys. Res., **103** (C4), 8045-8057.

Maes, C., and D. Behringer, 2000: Using satellite-derived sea level and temperature profiles for determining the salinity variability: A new approach, J. Geophys. Res., **105**, 8537– 8547.

McPhaden, M. J., T. Delcroix, K. Hanawa, Y. Kuroda, G. Meyers, J. Picaut, and M. Swenson, 2001: The El Niño/Southern Oscillation (ENSO) Observing System. *Observing the Ocean in the 21st Century,* C. J. Koblinsky and N. R. Smith, Eds., Australian Bureau of Meteorology, 231–246.

Pacanowski, R.C. and S. M. Griffies, 1998: MOM 3.0 Manual. NOAA /Geophysical Fluid Dynamics Laboratory, Princeton, NJ, USA 08542.

Reynolds, R. W., N. A. Rayner, T. M. Smith, D. C. Stokes and W. Wang, 2002: An improved in situ and satellite SST analysis for climate. J. Climate, **15**, 1609-1625.

Saha, S., S. Nadiga, C. Thiaw, J. Wang, W. Wang, Q. Zhang, H. M. van den Dool, H.-L. Pan, S. Moorthi, D. Behringer, D. Stokes, G. White, S. Lord, W. Ebisuzaki, P. Peng, P. Xie, 2005: The NCEP Climate Forecast System. *Submitted to J. Climate.*

Vossepoel, F. C. and D. W. Behringer, 2000: Impact of sea level assimilation on salinity variability in the western equatorial Pacific. J. Phys. Oceanogr., **30**, 1706-1721.